Sustainable district energy integrating biomass peaking with geothermal baseload heating: A case study of decarbonizing Cornell's energy system

Cite as: J. Renewable Sustainable Energy **12**, 066302 (2020); https://doi.org/10.1063/5.0024841
Submitted: 11 August 2020 . Accepted: 15 November 2020 . Published Online: 22 December 2020

Nazih Kassem, James Hockey, Steve Beyers, Camilo Lopez, Jillian L. Goldfarb, Largus T. Angenent, and Jefferson W. Tester

Journal of Renewable and Sustainable Energy ARTICLE scitation.org/journal/rse

Sustainable district energy integrating biomass peaking with geothermal baseload heating: A case study of decarbonizing Cornell's energy system

Cite as: J. Renewable Sustainable Energy **12**, 066302 (2020); doi: 10.1063/5.0024841
Submitted: 11 August 2020 · Accepted: 15 November 2020 ·
Published Online: 22 December 2020

Nazih Kassem,[1,2,a)] James Hockey,[2] Steve Beyers,[3] Camilo Lopez,[4] Jillian L. Goldfarb,[1,2] Largus T. Angenent,[5] and Jefferson W. Tester[2,6]

AFFILIATIONS

[1]Department of Biological and Environmental Engineering, Riley Robb Hall, Cornell University, Ithaca, New York 14853, USA
[2]Cornell Energy Systems Institute, Cornell University, Ithaca, New York 14853, USA
[3]Cornell Facilities Engineering, 201 Humphreys Service Building, Cornell University, Ithaca, New York 14853, USA
[4]Electrochaea GmbH, Semmelweisstraße 3, 82152 Planegg, Germany
[5]Centrum for Applied Geosciences, University of Tübingen, Schnarrenbergstraße 94-96, 72076 Tübingen, Germany
[6]School of Chemical and Biomolecular Engineering, Olin Hall, Cornell University, Ithaca, New York 14853, USA

[a)]Author to whom correspondence should be addressed: nk644@cornell.edu

ABSTRACT

Many governments and institutions are advocating for higher renewable energy deployment to lower their carbon footprint and mitigate the effects of climate change. Cornell University instituted the "climate action plan" to achieve carbon neutrality, of which geothermal heat extracted from deep rocks (Earth source heat) is a critical component. This paper proposes coupling baseload geothermal heating with energy from waste biomass from Cornell's dairy farms to meet the campus' peak heating demand. The envisioned biomass peaking system, consisting of a hybrid anaerobic digestion/hydrothermal liquefaction/biomethanation process, produces renewable natural gas (RNG) for injection and storage into the natural gas (NG) distribution grid and uses NG withdrawals at times of peak heating demand. We show that 97% of the total annual peak heating demand (9661 MW h) can be met using continuous RNG production using manure from Cornell's 600 dairy cows, which provides 910×10^6 l of RNG/year. The overall RNG system requires \$8.9 million of capital investment and, assuming favorable policies, could achieve an effective levelized cost of heat (LCOH) of \$32/GJ (minimum RNG selling price) and a net present value of \$7.5 million after a 30-year project lifetime. Favorable policies were quantified by examining a range of incentivized prices for RNG injection (\$47/MJ) and assuming wholesale utilities costs (NG withdrawals and electric imports). Selling RNG at the New York commercial NG price (\$7/GJ) with utilities imports at commercial rates produces an LCOH (\$70/GJ) in excess of the RNG selling price, highlighting the importance of carbon credits for financial profitability.

I. INTRODUCTION

Governments and institutions (public and private alike) are advocating for greater renewable energy deployment to lower their carbon footprint and mitigate the effects of climate change. Individual states have focused on electrifying the grid with renewable sources to replace fossil energy.[1–3] In New York state (NYS), home to Cornell University (Cornell), an initiative called reforming the energy vision (REV) was launched in 2019 to develop new energy products and services and protect the environment while increasing the state's economic prosperity.[4] REV's specific clean energy and climate goals include an 85% reduction in greenhouse gas (GHG) emissions by 2050 (from 1990 levels), 100% clean electricity by 2040 (Fig. 1), and increased deployment of distributed energy resources such as offshore wind, solar, and energy storage.

While the portion of renewable electricity generation from wind and solar photovoltaic (PV) in New York is increasing, conventional hydropower is still the major source of carbon-free renewable electricity at 22% of net electricity generation. Wind and solar (combined) represent only about 5%, while nuclear and natural gas (NG) represent around 28% and 44% of the total electric power supply, respectively.[5]

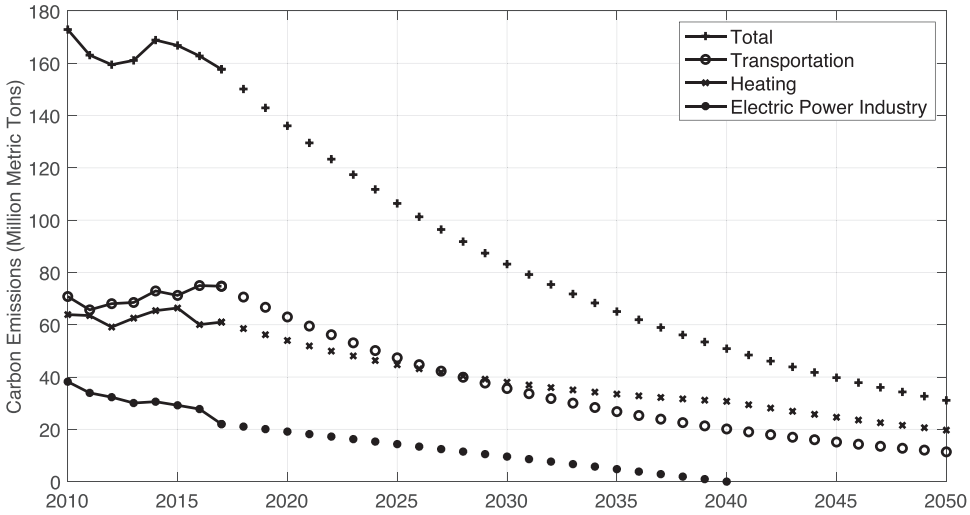

FIG. 1. Historic and projected carbon emissions in New York state by energy sectors. Solid lines are historical emissions. Dotted lines are predictions estimated assuming a hypothetical carbon mitigation model: the total and electric emissions predictions are based on REV climate goals, transportation emission reduction targets were based on California's policy to cut oil use for transportation by half by 2030,[11] and heating emissions were interpolated by the difference between the total and transportation and electric power emissions. (Data source: EIA, 2017).[12]

While increasing renewable electric power deployment is important to lower carbon emissions, it does not directly address carbon emissions associated with providing heat for buildings and industrial processes. Moreover, there is a high demand for heating in NY, which is a northeastern state that experiences long, cold winters. A large portion of primary energy consumed in this region is for heating purposes; around 35% of NYS's carbon footprint results from consuming natural gas, heating oil, and propane to heat its residential, municipal, and commercial buildings.[6–10] Low-temperature industrial heat accounts for an additional 10% of the total carbon footprint in NYS.

The hypothetical carbon emission reduction trajectory in NYS, based on REV's goals and on an assumed 50% reduction in transportation emissions, is plotted in Fig. 1.

To achieve its climate goals, New York state must reduce its heating sector carbon intensity by at least two thirds by 2050, from 2017 levels (Fig. 1). Reducing heating carbon intensity can be achieved by using renewable electricity to supply heat via direct resistance heating, or more efficiently, with the use of air source or ground source heat pumps. However, these techniques are typically deployed in individual or small clusters of buildings, and they require electricity, which would have to come from carbon free sources, such as solar PV or wind. To achieve carbon neutrality in regions with large annual heating demands, a significant increase in renewable electric generating capacity from solar and wind is required, imposing major land use and economic limitations, and increasing the burden on electric power demand during winter periods. Additionally, heat pump refrigerants, which are themselves significant greenhouse gas contributors, would have to be well managed to see a net benefit.[13,14] An alternative to more sustainably achieving NYS's REV goals for lowering carbon emissions would be to utilize renewable geothermal and bioenergy resources deployed at community scales in distributed district energy systems. Recognizing the inherent land use limitations of sustainable biomass production,[15–17] the option of using biomass for peak heating is much more feasible than for providing baseload heat. Geothermal, on the other hand, is ideal for baseload district energy supply with its small land-use requirement and inherent dispatchability.[18–20]

Located in Ithaca, NY, Cornell experiences long winters, often lasting 5–6 months with over 6971° days of heating (base 65) in 2019.[21] Ithaca's annual average temperature is about 7 °C and as such, heating represents a significant portion of Cornell's on-campus energy usage, with peaks reaching 80 MW_{th} (supplementary material, Sec. I). In 2009, Cornell developed the climate action plan (CAP) as a roadmap to achieve carbon neutrality, detailing action points to develop new energy solutions and reduce campus emissions[22] (Fig. 2 and supplementary material, Sec. II). To eliminate the use of natural gas combustion for campus heating, Cornell is developing the Earth source heat (ESH) geothermal district heating demonstration project, which uses enhanced geothermal system (EGS) technology to provide baseload heating.[23,24] The low end-use temperatures required for heating buildings and supplying hot water are widely found at technically accessible depths underground ranging from 3 to 4 km, making EGS an ideal low-carbon, low-land use alternative for baseload heating.[24]

The goal of this study is to evaluate the technical and economic feasibility of a renewable biomethane system to meet the peak heating demand of Cornell's Ithaca campus. We propose a hybrid anaerobic digestion (AD) and hydrothermal liquefaction (HTL) system to convert dairy manure from Cornell's dairy farms into renewable natural gas (RNG). AD is a biological process that converts organic matter into biogas (CO_2 and CH_4). The liquid digestate, a by-product of the AD process, contains significant amounts of carbon that could be converted further into valuable fuels and chemicals. HTL has been proposed as a secondary processing step, converting the digestate into biocrude oil and hydrochar. To increase methane output, and thus the ability to meet Cornell's peak heating demand, we investigated the integration of the hybrid AD–HTL system within a power-to-gas (PtG) framework[25–28] using a novel biomethanation (BM) process. The PtG system converts renewable electricity and CO_2 (sourced from AD and HTL) into additional methane (RNG) (Fig. 2). As such, the chemical storage of excess renewable and intermittent electricity[29,30] using carbon capture and utilization technologies (CCU) becomes more attractive as the share of renewables in the electric power sector increases. This highlights the need for techno-economic assessments to guide the development and deployment of such technologies.[31] In this study, RNG is generated continuously (as opposed to the intermittent nature of solar and wind electric supply) and injected into the natural gas grid, at a premium, for storage and later use during peak

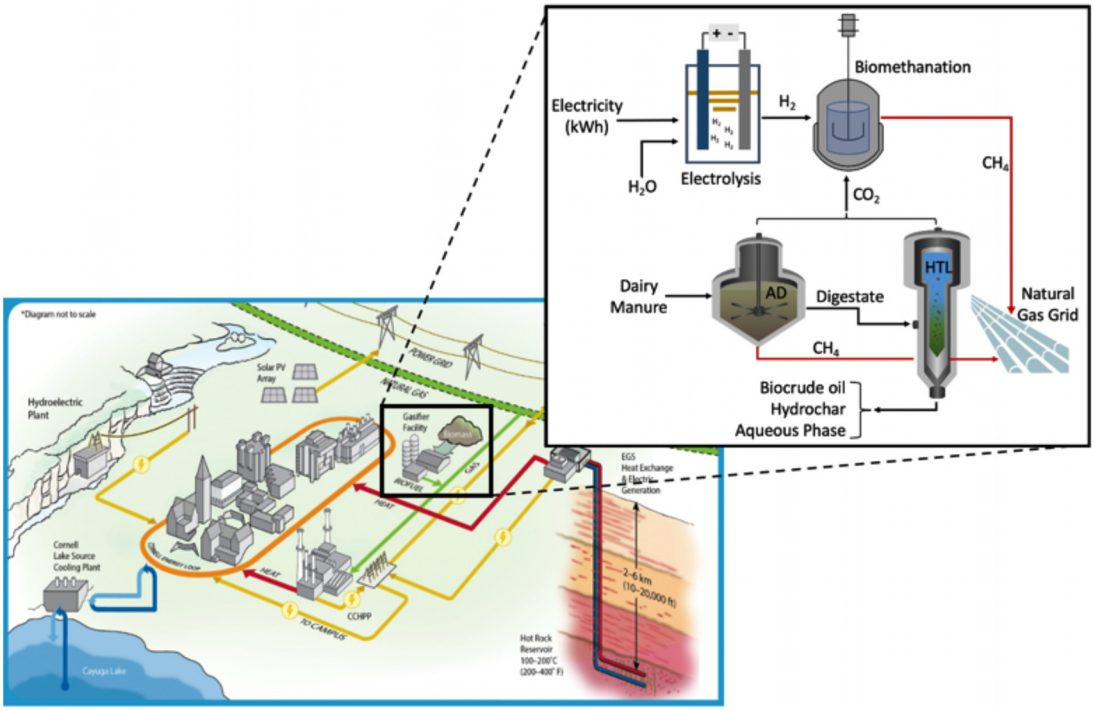

FIG. 2. Process flow diagram of the proposed Cornell biorefinery system including AD, HTL, and PtG biomethanation, and its integration within the Cornell University campus planned energy infrastructure.

demand periods. The treatment of injected RNG financially is analogous to feed-in tariffs (FITs) where utilities purchase renewable electricity from power producers at rates well above retail prices, using long-term contracts.[32] Finally, we propose the use of the low carbon fuel standard (LCFS) and renewable fuel standard (RFS) to obtain initial estimates for FIT prices.

Numerous studies have assessed the techno-economic feasibility of PtG systems. Collet *et al.*,[33] Vo *et al.*,[34] and Van Dael *et al.*[35] evaluated an integrated AD–BM system, but none have considered digestate processing. Michailos *et al.*[36] use gasification as a post-AD step in a wastewater treatment context. In heating dominated regions such as NY, a number of renewable heating options are being considered to decarbonize the region's energy footprint. The novelty of our study lies in the systems integration of RNG peak heating with geothermal baseload district heating, using a three-step biological–thermochemical–biological (AD–HTL–BM) processing approach. A successful demonstration of the ESH–biomass system could catalyze the deployment of hybrid geothermal-biomass heating systems in New York and other northern states with high heat demands,[24] contributing to state-wide efforts in meeting the REV climate goals.

II. MATERIALS AND METHODS

A. System boundaries and scope

The cow manure feedstock is available from the teaching dairy barn on campus and the dairy research center situated off-campus. Together, the facilities house around 600 dairy cows, with a capacity to add 200 more. Each dairy cow is assumed to produce 68 l of wet manure per day.[37] Both facilities are configured as concentrated animal feeding operations (CAFOs), facilitating the collection and storage of manure. Cornell's CAFOs are somewhat smaller than most in NYS but operate similarly. To establish a net greenhouse gas emissions framework, the system was bounded by the electric power source and the AD biogas production at the input level (carbon burdens and benefits from the electric source and avoided manure methane emissions, respectively) (supplementary material, Sec. V) and the natural gas grid at the output level (avoided emissions due to NG displacement). Two electricity sources were evaluated in this study: the NYS electric grid, based on its average fuel mix,[5,38] and a hydroelectric power purchase agreement. Manure transportation emissions were accounted for separately.

The coordinates of the compressed natural gas (CNG) compressor station that is nearest to the proposed biorefinery were obtained from the EIA US Energy Information Mapping system,[39] while those of the teaching dairy barn and dairy research center were obtained from the Cornell department of Animal Science facilities website.[40] The plant was sited near Cornell's main campus (Fig. 3), where it could serve as a demonstration plant for larger scale implementation prospects. The proposed plant is located on an empty plot about 2 km east of the central campus, about 200 m away from the teaching dairy barn (which houses 160 cows), and about 4 km from the compressor station. The proximity of the proposed biorefinery to the heat demand center, teaching dairy barn, and compressor station reduces transmission losses, manure transportation, and RNG piping distances. The dairy research center, which houses 440 dairy cows, is situated in Harford, which is about 17 km east of the campus. The relative distances between system components were estimated using Google Maps.

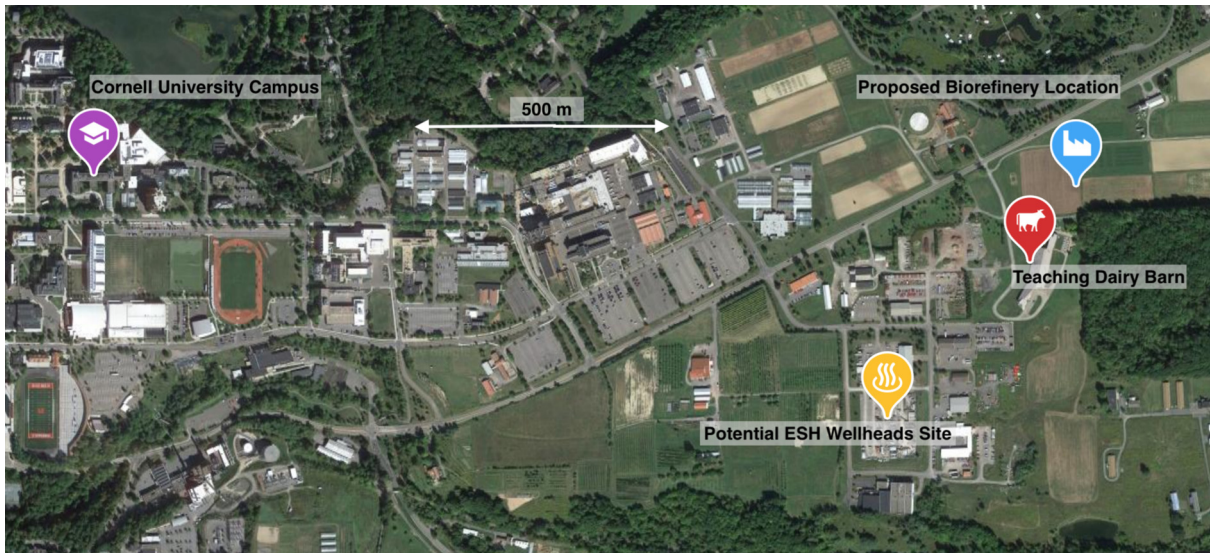

FIG. 3. Relative location of the proposed biorefinery with respect to the Cornell campus, the teaching dairy barn, and the potential ESH wellheads and heat exchangers connecting to Cornell's district heating system.

B. Heat load data and estimation of peak heating requirements

Heat load data for the Cornell campus for the 2017 fiscal year were obtained from the Earth source heat (ESH) project. The data consist of the hourly heat loads for the period starting June 18, 2016 at 12:00 am through June 17, 2017 at 12:00 am. The total hourly heat load consists of heat sales (MW_{th}) as read by building meters. The baseload heating will be provided by the planned geothermal ESH system. The ESH system consists of a set of geothermal wells and heat exchangers augmented with heat pumps to provide 50 MW thermal of the total heat output. For each hour, the remaining heat load (peak load) to be provided by RNG is calculated by subtracting 50 MW from the total heat requirement for that hour. The annual total peak heat demand supplied by RNG is calculated by integrating the hourly peak heat loads over the period of peak heating throughout the year as follows:

$$Q = \int_0^h (Heat\ sales_h - 50\,\mathrm{MW})dh, \tag{1}$$

where Q is the annual total heat load to be supplied by RNG in MW $h_{thermal}$ and h represents the hours when a peak load occurs (i.e., where heat sales >50 MW).

C. Operating conditions and model assumptions

1. Anaerobic digester and hydrothermal liquefaction process units

AD is a biological process mediated by mesophilic bacteria where biomass is converted into biogas (methane and carbon dioxide) via a series of hydrolysis and fermentation reactions.[41,42] Biogas can either be combusted using combined heat and power or upgraded to biomethane.[43] The digestion process is relatively slow compared to physio/chemical conversions, with retention times up to 6 weeks, depending on the digester type and feedstock composition and solid content.[41,44–46] AD is a well characterized process with proven benefits in terms of reducing GHG emission and nutrient runoff[47,48] compared to direct land spreading of raw manure. Manure digestate, which is a by-product of the digestion process, can be used as a soil amendment if land-applied in a sustainable manner (non-excessive application). Although AD reduces the amount of pathogens in manure, the degree of removal depends on a multitude of factors such as resistance of some pathogens to the digestion process, processing temperatures, residence times, and feedstock composition.[49] As such, additional steps are necessary to sterilize the digestate and eliminate all pathogens. Furthermore, the digestate contains a significant amount of carbon that can be converted into valuable fuels and products. The proposed AD was assumed to operate at a mesophilic temperature of 35 °C (Ref. 41) with a hydraulic retention time (HRT) of 20 days. The digester system was sized at 979 m^3 (which includes 20% extra headspace) to handle the daily manure flow produced by Cornell's 600 dairy cows (40 800 kg/day of wet manure with 87 wt. % moisture content). The AD model computes methane generation (biomethane) using a methane yield of 264 l CH_4/kg VS (VS: volatile solids).[50] A carbon mass balance was developed to compute digestate generation. Manure digestate has a 93 wt. moisture content and consists of the undigested organics and fixed solids.

Hydrothermal liquefaction (HTL) is a potential post-AD step to thermochemically treat the manure digestate. Unlike AD, HTL uses high temperature and pressurized water to convert organics into biocrude oil, hydrochar, and other value-added chemicals following a series of dehydration and condensation reactions.[51] HTL also produces an aqueous phase containing dissolved organic compounds and a gaseous stream consisting mainly of CO_2.[51] The hydrothermal liquefaction plant was assumed to run continuously, with an operating temperature of 300 °C and a 60 min residence time. Given a manure

digestate input flow rate, the HTL mass balance model computes co-product generation using carbon conversion yields given by Posmanik *et al.*[51] Biocrude oil can be sold as an alternative fuel to petroleum refineries[52] and hydrochar, if shown to have similar characteristics to biochar, could be used as a soil amendment to improve soil fertility[53–55] and retain water,[56] reducing potential environmental problems associated with nutrient runoff. The aqueous phase can be further processed to recover nutrients; however, this is beyond the scope of this study. Details pertaining to the AD and HTL mass balance models (assumptions and parameters) can be found in an earlier publication by our group.[57]

2. Electrolyzer and biomethanation components

Hydrogen can be produced from a variety of primary energy sources and technical processes[58] such as alkaline,[59] proton membrane,[60,61] or solid oxide electrolysis.[62,63] In this study, alkaline water electrolysis (AEL) with 70% average efficiency [High Heating Value (HHV)-based] was used for hydrogen production because of its maturity[64] and commercial prevalence.[65–67] The water required for electrolysis was assumed to be sourced from Beebe and Cayuga lakes near the campus, and was assumed to be filtered and de-ionized using capacitive deionization (CDI).[68] The biomethanation process uses Electrochaea's BioCat system,[69] where selectively evolved *archaea* catalyze the conversion of renewable hydrogen and carbon dioxide into methane (e-methane) and water, according to the following overall stoichiometric reaction with a reported 99% stoichiometric efficiency for the conversion of CO_2 into CH_4 [80% energy (HHV) based][47,57]

$$CO_2 + 4H_2 \rightarrow CH_4 + 2H_2O.$$

The biomethanation process in this study occurs *ex situ*, where carbon dioxide generated by AD and HTL would be fed into a separate reactor.[70,71] The water produced can be treated and re-injected into the lakes or used for irrigation; the processing and use of the water is beyond the scope of this study. The PtG system capacity is rated in MW_e and estimated based on the total CO_2 production assuming complete conversion to methane as shown in the above reaction. This yields the amount of hydrogen to be produced, and thus, electric energy required for electrolysis. Using Electrochaea's capacity curve estimates, a 1 MW_e system converts 50 Nm^3/h of CO_2 into CH_4 as follows:[47,57]

$$PtG(MW_e) = \frac{x}{50}, \tag{2}$$

where x is the CO_2 flow rate (Nm^3/h) being fed to the methanation reactor and $PtG(MW_e)$ is the PtG system's capacity in megawatts electric.

D. Economic analysis assumptions

1. Capital and operating costs

The AD capital and operating costs were calculated using the "AD Budget Calculator V48" developed by the USDA's Economic Research Service.[72] The software also provides the costs of the CNG infrastructure required to process and upgrade biogas for pipeline injection. CNG operating costs include RNG pipeline transportation and is a function of distance piped. Costs are mainly a function of herd size. The software considers AD construction costs, pre-digester separation, biogas separation, mechanical building, and H_2S scrubbing (water-wash),[72–75] among others.

HTL is a relatively new technology in the early stages of development, with only pilot and lab scale systems built.[52,76–78] The HTL system consists of the reactor, heat exchangers, product separation, and pumping systems. Individual costs associated with each component were obtained from Van Doren *et al.*[77] The lack of cost data at commercial scale leads to considerable uncertainty in scaling costs to larger plant sizes. As such, HTL capital and operating costs were estimated using non-linear cost-curves accounting for economies of scale[79,80] as described in the following equations:

$$\frac{CC(HTL)_x}{CC(HTL)_{200}} = \left(\frac{x}{200}\right)^{0.6}, \tag{3}$$

$$\frac{OM(HTL)_x}{OM(HTL)_{200}} = \left(\frac{x}{200}\right)^{0.6}, \tag{4}$$

where x is the dry flow rate (kg/h) entering the HTL reactor, $CC(HTL)_x$ and $OM(HTL)_x$, the capital and O and M costs ($) of the HTL reactor at a dry flow rate x (kg/h), and $CC(HTL)_{200}$ and $OM(HTL)_{200}$, the total capital and annual operating costs, at a flow rate of 200 (kg/h) equal to $3 692 000 and $611 600, respectively.[77]

The electrolyzer and methanation plant capital costs were computed using Electrochaea's cost-curve estimates (supplementary material, Sec. III). Cost data were based on Electrochaea's BioCat methanation system and proprietary biocatalyst. These estimates do not include interconnection and civil works' costs which can vary depending on site specifics. Fixed operating costs for the electrolysis and biomethanation units were set at 3% of their respective capital costs. The total deionization cost of $0.25/$m^3$ was taken from Liu *et al.*,[68] which includes capital costs for equipment, ion exchange membrane and electrode replacement costs, and electricity and maintenance costs. Costs for maintenance and replacement of electrodes assumed an electrode lifespan of 0.5 years.

2. Transportation costs

Manure transportation from the Harford Farm to the on-campus biorefinery is assumed to be handled by a contracted private waste hauler. The Harford Farm is located 17 km away from the proposed biorefinery location. Manure transportation costs were estimated using an $82/h rate[81] for a driver and a 6000-gal truck, according to the following equation:

$$Annual\ transport\ cost = \frac{\$82}{\text{hours}} \times \frac{\text{hours}}{trip} \times \frac{trips}{\text{year}}, \tag{5}$$

where the number of hours per truck trip is calculated by considering the driving time (function of travel distance and average truck speed), loading/unloading time and accounting for 20 min for setting up the pumping equipment. The number of truck trips per year is calculated by dividing the annual manure production rate (gal/year) by the truck size (gal). Transportation costs from the teaching dairy barn were assumed to be negligible (<200 m transportation distance) and were not considered in the analysis. Manure transportation CO_2 emissions were calculated using a fuel efficiency of 5.82 mpg for class 7 and

8 trucks running on gasoline,[82] and a gasoline carbon intensity of 8.89 kg/gal.[83]

3. Utility operating costs

Utility costs include the costs for purchased electricity to power the electrolysis process and for natural gas needed to meet Cornell's peak heating demand. Cornell owns and operates its own pipeline tied to the primary regional pipeline which is owned and operated by Dominion Energy, and contracts for gas purchases based on a complex arrangement of day-ahead and fixed rates. Such rates (marginal rates) averaged a little less than $2.8/GJ over the past few years.[84] The NG Henry Hub spot price (wholesale) in Q4 2019 was $2.3/GJ.[84] However, to cover brokerage fees, annual pipeline maintenance, and inspection fees, Cornell charges its users a higher rate closer to the commercial value, which is around $7/GJ in NYS.[85] To make this study more applicable for other institutions with no NG assets in general, we used the commercial NG rate for the base case. The Cornell-specific case using the NG wholesale rate was evaluated as part of the sensitivity analysis.

Cornell currently generates its own electricity mostly from natural gas with a mix of renewables (hydro, solar). In this study, we assumed a case where sufficient renewable electricity would be sourced from the New York Power Authority's (NYPA) Niagara Power Project under a power purchase agreement (PPA). A fixed PPA price of $0.05/kW h was assumed based on average large-scale hydro plants' generation costs in the US and North America.[86–88] Currently, however, Cornell owns its own high-voltage substation and therefore has access to wholesale rates. Wholesale rates vary throughout the time of day and average between $0.03 and $0.04/kW h, based on 2018 hourly locational based marginal pricing (LBMP) data obtained from NYISO[38] (supplementary material, Sec. IV). Cornell charges its campus users a fixed rate of $0.08/kW h to cover substation investments and upgrading costs. For the same reasons stated earlier for natural gas, the 2019 NYS commercial electricity price of $0.14/kW h (Ref. 89) was considered for the base case. The renewable PPA and wholesale electricity rates were evaluated in the sensitivity analysis.

4. Biogas generation and RNG injection

In our model assumption, biogas from anaerobic digestion of dairy manure is continuously generated. Biogas is separated into its methane and carbon dioxide components using water scrubbing.[74] The electrolyzer is run in parallel to produce the hydrogen for the biomethanation process. Because of the physical and economic constraints of having gas storage tanks on-site, the total RNG produced is continuously injected into the natural gas grid for storage at a premium price using specified feed-in tariff (FIT) rates. During periods when heating demand exceeds geothermal baseload supply, natural gas purchased from the grid at commercial rates is used in existing auxiliary furnaces on campus to meet the peak demand. In this way, the continuous injection of RNG on average lowers the carbon intensity of the natural gas grid in an analogous way to how renewable electricity reduces the carbon intensity of the electric grid. The RNG profit is calculated by subtracting the annual NG costs from the annual RNG revenues:

$$NG_{cost} = commercial\ rate\left(\frac{\$}{\mathrm{MJ}}\right) \times annual\ peak\ heating\ demand\ (\mathrm{MJ}), \quad (6)$$

$$RNG_{revenues} = RNG\ produced\ (\mathrm{MJ}) \times RNG\ premium\left(\frac{\$}{\mathrm{MJ}}\right). \quad (7)$$

5. Renewable fuel pricing and carbon credits

Because New York state currently lacks specific policies to incentivize RNG pipeline injection, the magnitude and range of feed-in tariffs (FITs) for injected RNG are estimated using carbon credits from the renewable fuel standard (RFS) and California's low carbon fuel standard (LCFS). Under the RFS, renewable fuels are assigned a D-code based on pre-approved pathways used to produce the fuels.[90,91] Biomethane produced from cellulosic feedstocks, such as manures and agricultural digester residues, falls into the D3 RIN (renewable identification number) category (cellulosic biofuel), while biocrude oil falls under the D4 RIN category (biomass-based diesel). The e-methane produced from biomethanation does not fall under any of the RFS pre-approved production pathways, and as such, cannot be credited using the RFS. RFS premiums were estimated using Q4 2019 average D3 and D4 RINs credit prices.[92]

Credits generated under the LCFS are based on the carbon intensity (CI) (gCO_{2e}/MJ) of the renewable fuel. The LCFS, originally adopted in 2009, was developed to reduce the carbon intensity (CI) of transportation fuels consumed in California by at least 20% by 2030 from a 2010 baseline.[93] Therefore, to be eligible for credits under the LCFS, renewable fuels must be sold as transportation fuels, substituting for gasoline or diesel. For that purpose, RNG was priced as compressed natural gas (CNG) for use in CNG vehicles, as a replacement to conventional gasoline. Biocrude oil is assumed to be sold as a diesel substitute. The carbon credits are generated based on the difference between the CI of the renewable fuel relative to that of the conventional fuel it replaces (gasoline or diesel CI benchmark). We also propose a case (modified-LCFS) where the CI of RNG is compared to that of conventional NG in NYS, illustrating what a NYS-based carbon credit mechanism aimed at decarbonizing the NG heating sector could look like. The carbon allocation methodology for the integrated AD–HTL–BM system used to estimate the carbon intensity of the renewable fuels is detailed in Kassem *et al.*[57] Detailed RFS and LCFS credit calculations and fuel pricing methodologies can be found in Sec. V of the supplementary material. The final RNG and biocrude oil prices for the different electric power sources considered are tabulated in Table I.

Because of its water retention and nutrient availability properties,[94] hydrochar was assumed to be sold as a soil amendment rather than as a solid fuel. Hydrochar prices found in the literature were mainly based on breakeven production costs for hydrothermal carbonization (HTC) systems producing solid energy fuels as coal substitutes.[95,96] As such, the hydrochar selling price was computed based on average biochar prices in the US, equal to $2.74/kg.[97,98]

6. Cash flow analysis

A discounted cash flow (DCF) analysis was used to evaluate the financial profitability of our proposed peak heating system. The DCF,

TABLE I. Fuels selling prices. Selling price is composed of LCFS credit, RFS credit (if applicable), and fuel spot price. Values in parenthesis are calculated using the modified-LCFS.

Selling price ($/MJ)	Biomethane	e-methane	Biocrude oil
NY-grid power	0.043 (0.035)	0.033 (0.024)	0.051 (0.051)
Renewable power	0.053 (0.045)	0.042 (0.034)	0.061 (0.061)

incorporating capital and operating costs for the total investment of the biorefinery, was used to calculate financial indicators such as the net present value (NPV), levelized cost of heat (LCOH), and internal rate of return (IRR). The LCOH (in $/MJ) includes all costs incurred by the system (including annual and capital costs) to produce a MJ of RNG, and was calculated as follows:

$$LCOH = \frac{\sum_{t=1}^{n} \frac{I_t + M_t}{(1+r)^t}}{\sum_{t=1}^{n} \frac{E_t}{(1+r)^t}}, \quad (8)$$

where I_t, M_t, and E_t represent the investment expenditure, operation and maintenance costs, and methane energy generation in year t, respectively. The investment expenditure consists of the annualized initial capital cost throughout the project lifetime n. r represents the discount rate. For a better representation of economic performance, the effective LCOH ($LCOH_e$), corresponding to the minimum RNG selling price to breakeven at the end of the project lifetime, is computed by accounting for the system's revenue streams as follows:

$$LCOH_e = LCOH - R_h - R_b, \quad (9)$$

where R_h and R_b are the annual hydro-char and biocrude oil revenues normalized to the annual RNG output, respectively ($/MJ). The IRR is the discount rate (%) at which the project breaks even (NPV = 0) at the end of its project lifetime. The base case financial parameters assumed for the DCF are shown in Table II. Note that the tax rate is zero since Cornell is a not-for-profit institution and that two years of construction were accounted for in the DCF after which revenues start to be generated.

TABLE II. Base case financial parameters.

Tax rate	0%
Discount rate	5% (campus published standard rate)
RNG weighted average selling price[a]	$0.038/MJ
Project lifetime	30 years
Purchased electricity price	$0.14/kW h (NYS commercial rate)
Purchased NG price	$0.007/MJ (NYS commercial rate)
Biocrude oil price	$0.051/MJ ($1.42/l)
Hydrochar price	$2.74/kg

[a]Weighted by the volume of biomethane and e-methane.

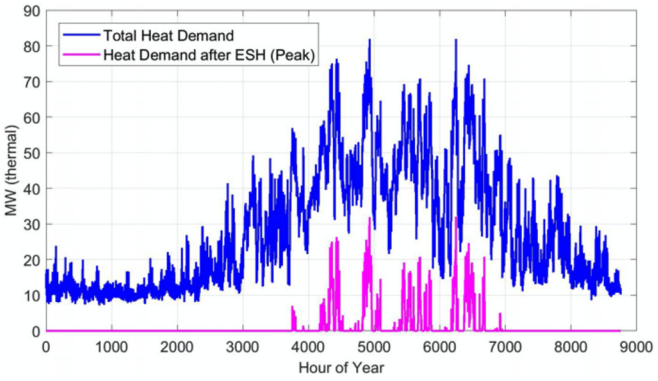

FIG. 4. Cornell campus' hourly heat load for the fiscal year 2017. Figure shows the total heat demand (blue) along with the peak heat demand (pink) remaining after the use of the 50 MW_{th} ESH for baseload heat. The peak heating demand will be provided by the proposed biomass system.

III. RESULTS AND DISCUSSION

The total yearly peak heat demand in 2017 was 9661 MW h_{th} (Fig. 4), spread over a total of 1076 h between November and April. The hybrid AD–HTL–PtG system produces around 909 × 10^6 liters of RNG per year, equivalent to 26 MW h_{th} of heat per day. Assuming continuous production throughout the year, the PtG system can provide 97% of the total annual peak heating demand, representing 80% of the peak heating hours (Fig. 5). The remaining 301 MW h_{th} required to meet the total peak heat demand can be met by purchasing natural gas, increasing Cornell's dairy herd size, or using campus eateries' food wastes for co-digestion. Adding 19 more dairy cows would result in enough RNG production to meet all the peak heating demand.

However, the 1076 h over which the peak heat demand is spread are not continuous and the peak heat loads distribution is not uniform

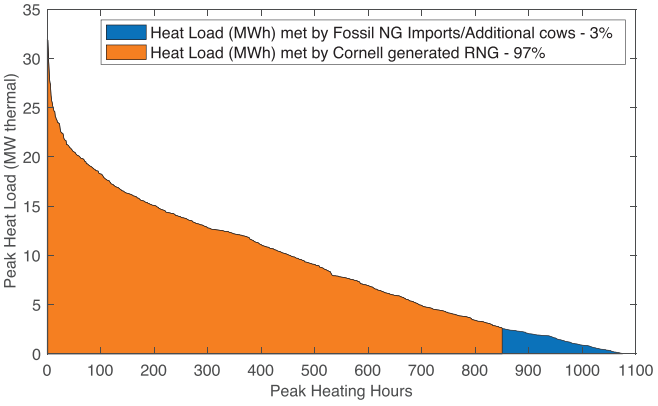

FIG. 5. Distribution of the 1076 peak heating hours (remaining after ESH) spread throughout the fiscal year 2017. Distribution is not continuous and is in descending order with respect to the peak heat load; it does not correspond to the passage of time throughout the year. The total peak heating demand—9661 MW h—is obtained by integrating the curve over the peak heating hours. Around 97% of the total peak heating demand could be met with Cornell-generated RNG, representing nearly 80% of the peak heating hours.

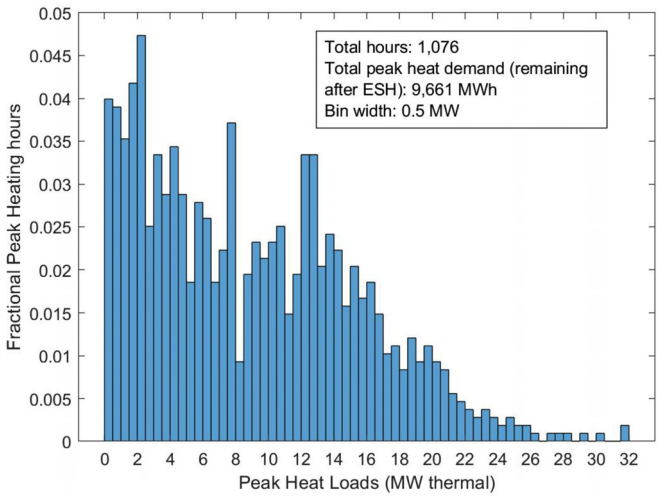

FIG. 6. Fractional peak heating hours as a function of peak heat loads (remaining after ESH) during the fiscal year 2017 plotted in the form of a frequency distribution function. Peak heat load bins are plotted in 0.5 MW increments. The total peak heating demand in 2017 was 9661 MW h (thermal) (35 TJ). Around 8% of the total peak heating hours have a heat load of 1.1 MW or less.

(Fig. 6), implying that for most of the extreme days, the daily RNG production would not be sufficient to meet the peak demand. Only about 8% of the peak hours, which have peak loads less than 1.1 MW_{th}, can be met with the hourly RNG production of 1.1 MW h (Fig. 6). The remaining hours have to be met using grid imports. On-site RNG storage would require a maximum storage capacity of 176×10^6 US gallons [calculated at ambient pressure and temperatures (NTP) by accounting for cumulative RNG production and peak heat loads]. As mentioned earlier, because of the physical size and associated capital costs of gas storage, it was not considered in this study. Instead, Cornell relies on the NG grid for storage, as depicted in Fig. 7. The biomass system is therefore not independent of the NG grid, in the same way that intermittent renewable electricity depends on the electric grid when it cannot meet the demand. RNG prices in the range shown in Table I are 5–8 times (depending on electricity source and RNG type) higher than the NYS NG commercial rate ($7/GJ). Under the modified LCFS, prices are still 3–6 times higher. Injecting RNG into the grid at the base case RNG weighted average price (by volume of biomethane and e-methane produced) of $38/GJ generates around $1.2 million per year. Profits generated could contribute toward paying the capital and operating costs of the required equipment. The hybrid AD–HTL–PtG system produces around 218 000 l of biocrude oil and 131 000 kg of hydrochar per year, equivalent to $309 000 and $360 000 of revenues, respectively.

A total of $8.9 million of capital investment is required to implement the hybrid peak heating system (Table III). The HTL reactor and CNG infrastructure represent the bulk of the total capital costs, with 31% and 29% of the total capital costs, respectively (Table III). The high CNG costs are mainly associated with interconnection costs, pipeline construction, permitting, and right of way costs, altogether representing around 79% of CNG capital costs. As for the HTL plant, heat exchangers represent a significant portion of total capital costs, with around 60% of the total. AD capital costs represent 20% of the total system capital costs (Table III). The higher cost of HTL compared to AD is explained by the conservative approach used to account for uncertainties in scaling up the HTL reactor, whereas AD is a relatively mature technology with known costs and economies of scale as a result of large-scale deployment. The PtG system, composed of the biomethanation plant and electrolyzer unit account for the remaining 20% of the total capital costs.

The total annual costs for the system were evaluated at $2.2 million (Table III) for the base case. HTL annual operating costs represent 21% of the total and are mainly due to the high heating requirements. Some of these costs may be offset in the future by utilizing available thermal energy from Cornell's district heating system. Using a commercial electric rate of $0.14/kW h, purchased electricity represents around 60% the total annual costs. This is mainly due to the large power requirement of the electrolyzer, at 9491 MW h_e annually. The

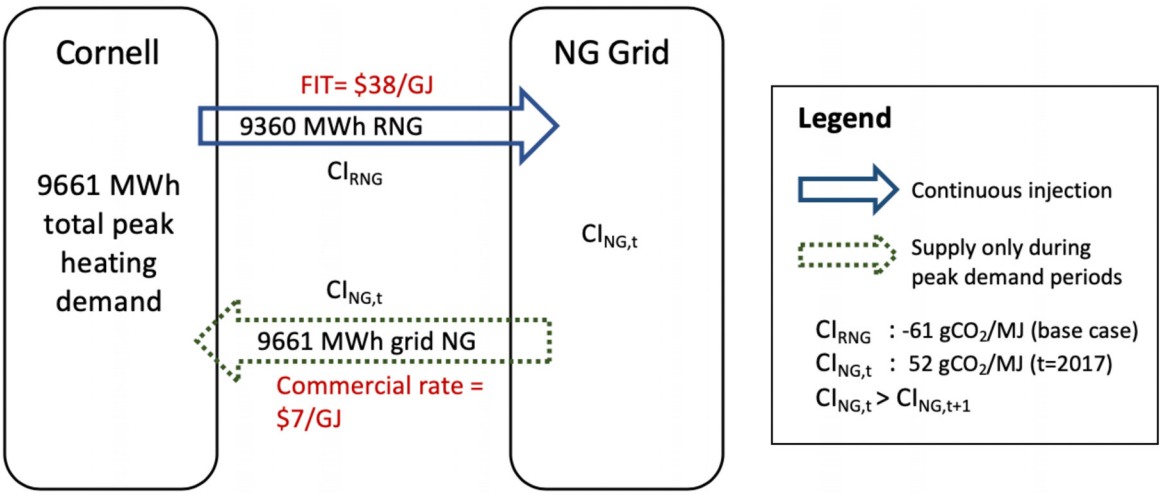

FIG. 7. RNG pricing and injection mechanism showing the NG flows between Cornell and the grid. The carbon intensity of the NG grid at year t ($CI_{NG,t}$) decreases incrementally as t increases, reflecting the partial grid decarbonization with continuous RNG injection.

TABLE III. Total capital and annual operating costs required for the proposed Cornell biorefinery system.

Component	Capital costs ($)	Annual operating costs ($)
Hydrothermal liquefaction	$2 782 600	$460 900
Anaerobic digestion	$1 761 900	$9800
CNG infrastructure	$2 615 500	$46 800
Biomethanation	$758 400	$22 800
Electrolysis	$975 000	$29 300
Transportation	…	$54 600
Electricity imports	…	$1 327 900a
Grid NG imports	…	$243 900[a]
Water deionization	…	$714
Total	$8 893 400	$2 196 714

[a]Based on base case parameters.

grid NG imports at commercial rates constitute around 11% of total annual costs. The remaining 8% are divided between the AD, CNG, biomethanation, electrolysis, water deionization, and transportation. Using the base case parameters (Table II), the total annual costs exceed the total annual revenues from RNG, biocrude, and hydrochar, resulting in yearly losses.

Under the base case conditions, a negative $12.6 million NPV at the end of the project lifetime of 30 years is calculated, with an LCOH of $83/GJ [Fig. 8(f)]. The effective LCOH ($LCOH_e$) accounting for biocrude oil and hydrochar revenues was in this case calculated to be

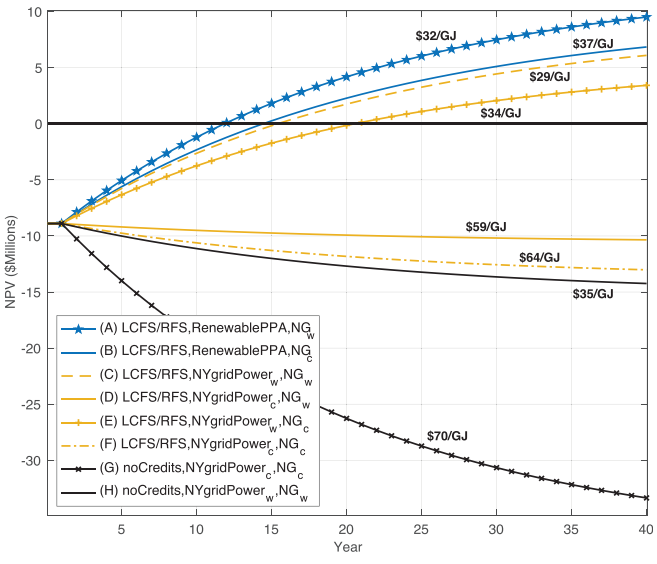

FIG. 8. NPV curves for different renewable fuels and utility pricing conditions. The legend items are in the format "renewable fuel (RNG and biocrude oil) pricing, purchased electricity source and pricing, and purchased natural gas (NG) pricing." Subscripts w and c denote "wholesale" and "commercial" rates. With "no credits," RNG is sold at the NG commercial price ($7/GJ). "LCFS and RFS" prices, which depend on the electricity source, are taken from Table I. The values displayed on the graph represent the $LCOH_e$.

$64/GJ. The $LCOH_e$, which corresponds to the break-even RNG selling price, is around 9 times higher than the NYS NG commercial price of $7/GJ, highlighting the importance of having state incentives and subsidies. Under the base case parameters, where NG and electricity are imported at their commercial prices, the weighted average RNG premium selling price of $38/GJ calculated using LCFS and RFS credits is lower than the $LCOH_e$. Lower purchased electricity prices would increase the NPV and decrease the $LCOH_e$. For example, the NPV becomes positive ($2.1 million) when the wholesale price (LBMP) of $0.033/kW h is used for purchased electricity. The $LCOH_e$ in this case decreases by almost half to $34/GJ [Fig. 8(e)] and becomes slightly below the RNG selling premium ($38/GJ), suggesting a $4/GJ profit. Electricity pricing greatly impacts the profitability of the biomass system, as imported electricity can constitute between 27% and 60% of the system's total annual costs when purchased electric rates are varied from wholesale to commercial rates, respectively (given fixed purchased NG commercial rates). Reducing the NG purchase price also improves the NPV and $LCOH_e$, but at a lower effect. If NG is purchased at wholesale prices ($2.3/GJ) while electricity remains priced at its commercial rate ($0.14/kW h), the resultant NPV would equal negative $10 million with an $LCOH_e$ of $59/GJ [Fig. 8(d)].

If both NG and electricity are imported at their wholesale rates, as is the case at Cornell, the NPV at the end of the project lifetime of 30 years is $4.4 million [Fig. 8(c)], representing a 50% return on investment. In this case, the calculated IRR for the project is 8.7%, 1.7 times higher than the campus published standard rate, suggesting a financially attractive plan.[99] The LCOH was calculated to be $0.048/MJ, and is comparable to that obtained by Michailos *et al.*[36] ($0.044/MJ) in their study of an integrated PtG system using AD, gasification, and biomethanation. The calculated $LCOH_e$ in this case is $0.029/MJ [Fig. 8(c)], suggesting a $9 profit for every GJ of RNG injected into the grid at the LCFS/RFS premium ($38/GJ). Although the calculated $LCOH_e$ is almost three times higher than that of conventional NG combined cycle power plants ($0.010/MJ),[100] the biomass peaking system offers GHG reduction benefits that will make it more attractive in the long-term with decarbonization targets ahead. In their PtG study, Parra *et al.* state that using direct air CO_2 capture increases the levelized cost of energy (LCOE) of their synthetic natural gas by $0.014/MJ compared to systems using biogas-sourced CO_2,[101] stressing the attractiveness of manure as a constantly available and no-cost feedstock. Other environmental benefits, such as odor reduction and nutrient runoff and groundwater contamination avoidance from manure land spreading, if quantified, could increase the attractiveness of the system. A local carbon and environmental credit program in NYS could increase the renewable fuel prices to competitive ranges that drive such bioenergy systems to profitability. Economies of scale enabled by bigger system sizes with higher waste throughput could greatly decrease the $LCOH_e$. The average $LCOH_e$ for a system of distributed AD–HTL–BM biorefineries in NYS treating manure from 397 000 cows was computed at $0.010/MJ.[57]

The source of electrical power used for electrolysis affects the profitability of the project. Using renewable electricity (as opposed to grid-sourced electricity) decreases the carbon intensity of the RNG and biocrude oil to −112 gCO_2/MJ each, down from −61 gCO_2/MJ using the NY electric grid (supplementary material, Sec. V), which increases their LCFS credits, and thus selling prices (Table I). Using hydroelectricity at an assumed PPA price of $0.05/kW h with NG

imports at the commercial rate results in a 30-year NPV of $5.1 million with an ROI of 57% and an IRR of 9.2%. The calculated $LCOH_e$ in this case is $37/GJ [Fig. 8(b)]. If NG is imported at a wholesale rate instead, the NPV would increase to $7.5 million, with an ROI, IRR, and $LCOH_e$ of 84%, 11%, and $32/GJ [Fig. 8(a)], respectively. In both cases, the RNG weighted average (biomethane and e-methane) selling price of $47/GJ calculated using LCFS and RFS credits is higher than the $LCOH_e$, highlighting the attractiveness of the system.

Without the use of carbon credits and assuming NG and electricity are imported from the grid at their commercial rates, the resultant NPV would equal negative $31 million [Fig. 8(g)]. Even if NG and electricity are imported using their wholesale prices, the NPV would still be negative at $13.6 million [Fig. 8(h)]. In both cases, RNG is assumed to be sold at the NG commercial rate ($7/GJ) and biocrude oil at the NY harbor ultra-low sulfur diesel (ULSD) spot price ($15/GJ). Furthermore, under the modified-LCFS, the RNG selling prices are decreased by 15%–30%, depending on the electric source and RNG type (Table I), resulting in reduced NPVs across all electricity and NG pricing configurations. This highlights the importance of having local carbon markets that incentivize RNG production within local energy contexts. If New York state were to adopt policies to create a carbon market and enable competitive RNG pricing, then the proposed biomass peak heating system would show profitability, with attractive NPV and ROI.

Some may question the validity of a premium RNG price assumption for pipeline injection over a longer term. To provide some perspective, it is important to keep in mind that the amount of RNG injected is very small relative to the annual consumption in NY state. More specifically, the total consumption of natural gas in NY state is about 1.3×10^{12} MJ/year (Ref. 102) vs 33×10^6 MJ/year (<0.003%) produced utilizing manure from Cornell's 600 dairy cows. Even if this method of producing RNG was deployed across the entire state's dairy CAFO farms which have about 400 000 cows, the total amount of RNG is 22×10^9 MJ/year (~2%).[57] While the economic and environmental benefits of utilizing dairy manure are potentially very large for farmers in dairy states like NY, CA, WI, and ID, disruptive impacts on supply of natural gas are minimal. This is in contrast to the disruptive impacts of intermittent renewables such as wind and solar that contribute a larger fraction of electric grid capacity in certain regions such as California.

To illustrate the comparative advantages of each individual process component, we evaluated the capital (CAPEX), operating expenditures (OPEX), NPV, breakeven period (BP), LCOH, RNG carbon intensity (CI), and RNG generation for four different configurations of anaerobic digestion (AD), hydrothermal liquefaction (HTL), and biomethanation (BM) (Table IV).

Given a fixed manure feed rate, the total system costs, consisting of capital and operational expenditures, increase with additional unit processes [Table IV(A)]. The AD-only system costs consist of the AD unit and CNG infrastructure. Adding HTL increases the CAPEX by $2.8 million, while adding a BM system increases the CAPEX by $1.2 million [Table IV(A)]. Including both HTL and BM adds $4.5 million in the CAPEX, which is $0.5 million higher than the sum of each incremental capital additions of the AD–HTL and AD–BM systems [Table IV(A)]. This is explained by the higher BM capacity from the increased CO_2 feed. The carbon intensity of RNG increases with the addition of unit processes. This is due to the allocation of carbon benefits of manure treatment to more energy products (biomethane, e-methane, and biocrude oil). As such, LCFS credits for RNG decrease with increased system complexity, resulting in lower selling prices. The decrease in RNG selling price is balanced by (1) increased RNG generation for systems with BM and by (2) biocrude oil and hydrochar generation for systems with HTL [Table IV(A)]. However, the table shows that for small-scale systems (600 cows), adding more process units does not result in higher financial returns. The NPV is in fact higher for an AD-only system and decreases as more unit processes are added. Similarly, the breakeven period is shorter for simpler systems. The LCOH, defined by the total system costs over total RNG generation (in GJ), increases with the addition of unit processes, since the increase in costs outweighs the increase in RNG generation for all cases. The magnitude of the increase is higher with the addition of HTL, since HTL increases total costs without generating additional RNG. However, the biocrude oil and hydrochar revenues generated with the addition of HTL can greatly reduce the effective levelized costs, as illustrated by the low $LCOH_e$ [Table IV(A)].

TABLE IV. Financial indicators and RNG carbon intensity and generation for different configurations of anaerobic digestion (AD), hydrothermal liquefaction (HTL), and biomethanation (BM). A 30-year lifetime was assumed in calculating the NPV and LCOH. The tabulated values were evaluated using renewable electricity and NG grid imports at their PPA ($0.05/kW h) and wholesale prices ($2.3/GJ), respectively, reflecting conditions available at Cornell (Fig. 8, case A).

Configuration	Number of cows	CAPEX ($ million)	OPEX ($ million)	NPV ($ million)	BP (years)	LCOH ($/GJ)	$LCOH_e$ ($/GJ)	RNG CI (gCO_2/MJ)	RNG generation ($MW h_{th}$)
(A) -Assuming fixed manure inflow									
AD	600	4.4	0.19	12.6	6	31	31	−276	4466
AD-HTL	600	7.2	0.65	12	8	71	19	−200	4466
AD-BM	600	5.6	0.57	9.8	8	34	34	−154	7980
AD-HTL-BM	600	8.9	1.2	7.5	12	53	32	−112	9360
(B) Assuming fixed RNG generation									
AD	1258	4.7	0.31	32	4	19	19	−276	9360
AD-HTL	1258	9.1	1	22.6	6	49	24	−200	9360
AD-BM	704	5.9	0.65	12.5	7	31	31	−154	9360
AD-HTL-BM	600	8.9	1.2	7.5	12	53	32	−112	9360

It is important to note that compared to an AD-only system, the amount of RNG generated increases with the addition of unit processes (AD–BM and AD–HTL–BM cases) [Table IV(A)]. Keep in mind that the values in Table IV(A) were calculated assuming the same manure feed rate (from 600 cows) in all configurations. Under this assumption, the RNG generated using the integrated AD–HTL–BM system (9630 MW h_{th}) is the closest in meeting the Cornell campus peak heating demand (9661 MW h_{th}). Table IV(B) illustrates the changes in costs, NPVs and LCOH values if all biorefinery configurations were to produce the same amount of RNG. To produce 9360 MW h of RNG, the cow count, and thus manure feed rate, has to increase by a factor of 2.1 for the AD and AD–HTL cases, and by 1.2 for the AD–BM case [Table IV(B)]. This is associated with slight increases in costs, and noticeably higher NPVs and lower LCOH values for the AD-only and AD–HTL configurations [Table IV(B)]. Overall, Table IV shows that for small-scale applications, peak heating systems with simpler configurations are more financially attractive. The interactions between the different configurations presented in Table IV provide useful information for farmers, industrial partners, and policy makers who are interested in evaluating the use of waste biomass for renewable heating applications, given a specified target energy (heat) requirement and limited available resources (capital and feedstock). Finally, although the biomass peak heating system relies on the NG grid for RNG storage, an increased deployment of large scale biomass-to-energy systems with RNG injection using dairy waste, and potentially food waste, would accelerate the partial decarbonization of the NG grid, which would in turn, decrease the carbon intensity of NG withdrawals over time (Fig. 7).

IV. CONCLUSION

This paper demonstrates how waste biomass could be effectively utilized to supply renewable natural gas (RNG) for peak heating of the Cornell University campus using an integrated anaerobic digestion—hydrothermal liquefaction—biomethanation system. Peak heating could be coupled to a baseload supply of thermal energy for Cornell's district energy system using geothermally heated water extracted from rock formations 3–4 km deep. This integrated use of geothermal heating and biogas from waste biomass helps reduce the carbon intensity of Cornell's energy system and the natural gas grid, and also provides revenue that can be used to offset the capital costs of purchasing and installing the AD–HTL–biomethanation system needed to produce the renewable biogas. The economic feasibility of this project hinges upon having favorable utilities (natural gas and electricity) import rates and state credit incentives available for RNG pricing. The lowest LCOH for the AD–HTL–BM system was achieved using NY grid electricity with wholesale utilities import rates, while the highest NPV was achieved using renewable power under a power purchase agreement (PPA) contract combined with natural gas wholesale imports. The highest LCOH values were obtained when commercial rates were used for utilities import, while the lowest NPV values were obtained when no carbon credits were used. In NYS, pressing environmental problems due to the mismanagement of agricultural wastes such as lake and river basin eutrophication and groundwater pollution, could push forward legislations that enable new environmental standards and regulations along with providing credit mechanisms that would drive up RNG prices. Finally, the integrated geothermal baseload/biomass peak heating system is a viable option for eliminating the substantial GHG emissions associated with campus heating, a key element of Cornell's CAP for achieving carbon neutrality by 2050. A successful demonstration of a renewable heating system at this scale could catalyze the deployment of integrated biomass-to-RNG systems in NYS and beyond, contributing in the partial decarbonization of gas grids and helping states and institutions meet their climate and energy goals. For example, with 29 CAFO farms housing 28 000 dairy cows located within 25 miles of Cornell, the local region would have a potential to become a waste-to-energy hub to substantially increase the production of renewable biogas and reduce the environmental impacts of dairy farms in the region.

SUPPLEMENTARY MATERIAL

See the supplementary material for additional information on Cornell University's climate action plan and carbon allocation and credit calculation methodologies, as well as data on Electrochaea's cost curves and NYISO pricing data.

ACKNOWLEDGMENTS

The authors thank Dr. Laurent Lardon and Mitch Heinz (Electrochaea, Munich, Germany) for their valuable contribution on carbon credits, Professor Thomas Overton, Professor Michal Moore, and Professor Lindsay Anderson for their helpful insights on dairy waste management and energy markets. Finally, we gratefully acknowledge the partial support provided by Cornell's Atkinson Center for a Sustainable Future, the Cornell Energy Systems Institute, and the US–Israel Binational Agricultural Research and Development (BARD) fund.

The authors declare no conflicts of interest.

DATA AVAILABILITY

The data that support the findings of this study are available within the article and its supplementary material.

REFERENCES

[1]B. J. Alqahtani and D. Patiño-Echeverri, "Combined effects of policies to increase energy efficiency and distributed solar generation: A case study of the Carolinas," Energy Policy **134**, 110936 (2019).
[2]M. Arbabzadeh, R. Sioshansi, J. X. Johnson, and G. A. Keoleian, "The role of energy storage in deep decarbonization of electricity production," Nat. Commun. **10**, 3413 (2019).
[3]H. Johlas, S. Witherby, and J. R. Doyle, "Storage requirements for high grid penetration of wind and solar power for the MISO region of North America: A case study," Renewable Energy **146**, 1315 (2020).
[4]See https://rev.ny.gov/ for New York State Government, Reforming the Energy Vision, 2019.
[5]See https://www.nyiso.com/real-time-dashboard for New York Independent System Operator, Real-time dashboard, 2020.
[6]See https://energyplan.ny.gov/-/media/nysenergyplan/2014stateenergyplan-documents/2015-nysep-vol2-enduse.pdf for New York State Energy Planning Board, The Energy to Lead—End-use Energy, 2015.
[7]K. McCabe, M. Gleason, T. Reber, and K. R. Young, "Characterizing U.S. heat demand for potential application of geothermal direct use," Trans. –Geotherm. Resour. Counc. **40**, 721 (2016).
[8]See https://www.eia.gov/consumption/commercial/data/2012 for Energy Information Administration, Commercial Buildings Energy Consumption Survey, 2012.

[9]See https://www.eia.gov/state/seds/seds-data-complete.php?sid=US#Consumption for Energy Information Administration, State Energy Data System (SEDS):1960–2016, 2018.
[10]See https://www.eia.gov/consumption/residential/data/2015/ for Energy Information Administration, Residential Energy Consumption Survey, 2015.
[11]See https://ww3.arb.ca.gov/cc/scopingplan/meetings/082018/august-20-2018-ghg-workshop-summary.pdf for California Air Resources Board, Opportunities for Additional Reductions from Petroleum Transportation fuels, 2018.
[12]See https://www.eia.gov/environment/emissions/state/ for Energy Information Administration, State Carbon Dioxide Emissions Data, 2017.
[13]A. Mota-Babiloni, J. R. Barbosa, P. Makhnatch, and J. A. Lozano, "Assessment of the utilization of equivalent warming impact metrics in refrigeration, air conditioning and heat pump systems," Renewable Sustainable Energy Rev. **129**, 109929 (2020).
[14]S. Bobbo, L. Fedele, M. Curcio, A. Bet, M. De Carli, G. Emmi, F. Poletto, A. Tarabotti, D. Mendrinos, G. Mezzasalma, and A. Bernardi, "Energetic and exergetic analysis of low global warming potential refrigerants as substitutes for R410A in ground source heat pumps," Energies **12**, 3538 (2019).
[15]M. V. A. Finco and W. Doppler, "Bioenergy and sustainable development: The dilemma of food security and climate change in the Brazilian savannah," Energy Sustainable Dev. **14**, 194 (2010).
[16]D. Thrän, T. Seidenberger, J. Zeddies, and R. Offermann, "Global biomass potentials—Resources, drivers and scenario results," Energy Sustainable Dev. **14**, 200 (2010).
[17]K. Vávrová, J. Knápek, and J. Weger, "Modeling of biomass potential from agricultural land for energy utilization using high resolution spatial data with regard to food security scenarios," Renewable Sustainable Energy Rev. **35**, 436 (2014).
[18]J. Pálné Schreiner and A. Csébfalvi, in Proceedings of the Thirteenth International Conference on Civil, Structural and Environmental Engineering Computing (2011).
[19]J. Tester, T. Reber, K. Beckers, M. Lukawski, E. Camp, G. Aguirre, T. Jordan, and F. Horowitz, "Integrating geothermal energy use into re-building American infrastructure," in Proceedings of the World Geothermal Congress (2015).
[20]J. G. Gluyas, C. A. Adams, J. P. Busby, J. Craig, C. Hirst, D. A. C. Manning, A. McCay, N. S. Narayan, H. L. Robinson, S. M. Watson, R. Westaway, and P. L. Younger, "Keeping warm: A review of deep geothermal potential of the UK," Proc. Inst. Mech. Eng., Part A **232**, 115 (2018).
[21]See https://fcs.cornell.edu/departments/energy-sustainability/energy-management-overview/energy-fast-facts for Cornell Facilities and Campus Services, Central Energy Plant Fast Facts, 2019.
[22]See https://sustainablecampus.cornell.edu/our-leadership/cap for Cornell University Sustainable Campus, Climate Action Plan, 2019.
[23]S. Beyers and O. Racle, in Proceedings of the World Geothermal Congress, Reykjavik (2020).
[24]J. W. Tester, S. Beyers, J. Olaf Gustafson, T. E. Jordan, J. D. Smith, J. A. Aswad, K. F. Beckers, R. Allmendinger, L. Brown, F. Horowitz, D. May, T. Ming Khan, and M. Pritchard, "District geothermal heating using EGS technology to meet carbon neutrality goals: a case study of earth source heat for the Cornell University campus," in Proceedings of the World Geothermal Congress (2020).
[25]M. R. Martin, J. J. Fornero, R. Stark, L. Mets, and L. T. Angenent, "A single-culture bioprocess of methanothermobacter thermautotrophicus to upgrade digester biogas by CO_2-to-CH_4 conversion with H_2," Archaea **2013**, 1.
[26]S. Schiebahn, T. Grube, M. Robinius, L. Zhao, A. Otto, B. Kumar, M. Weber, and D. Stolten, "Power to gas," in *Transition to Renewable Energy Systems*, edited by D. Stolten and V. Scherer (Wiley, 2013), Chap. 39, pp. 813–848.
[27]M. Götz, J. Lefebvre, F. Mörs, A. McDaniel Koch, F. Graf, S. Bajohr, R. Reimert, and T. Kolb, "Renewable power-to-gas: A technological and economic review," Renewable Energy **85**, 1371 (2016).
[28]K. Ghaib and F. Z. Ben-Fares, "Power-to-methane: A state-of-the-art review," Renewable Sustainable Energy Rev. **81**, 433 (2018).
[29]D. C. Rosenfeld, H. Böhm, J. Lindorfer, and M. Lehner, "Scenario analysis of implementing a power-to-gas and biomass gasification system in an integrated steel plant: A techno-economic and environmental study," Renewable Energy **147**, 1511 (2020).
[30]M. Bailera, P. Lisbona, L. M. Romeo, and S. Espatolero, "Power to Gas projects review: Lab, pilot and demo plants for storing renewable energy and CO_2," Renewable Sustainable Energy Rev. **69**, 292 (2017).
[31]A. W. Zimmermann, J. Wunderlich, L. Müller, G. A. Buchner, A. Marxen, S. Michailos, K. Armstrong, H. Naims, S. McCord, P. Styring, V. Sick, and R. Schomäcker, "Techno-economic assessment guidelines for CO_2 utilization," Front. Energy Res. **8**, 5 (2020).
[32]See https://www.eia.gov/todayinenergy/detail.php?id=11471 for Energy Information Administration, Feed-in tariff: A policy tool encouraging deployment of renewable electricity technologies—Today in Energy—U.S., 2013.
[33]P. Collet, E. Flottes, A. Favre, L. Raynal, H. Pierre, S. Capela, and C. Peregrina, "Techno-economic and Life Cycle Assessment of methane production via biogas upgrading and power to gas technology," Appl. Energy **192**, 282 (2017).
[34]T. T. Q. Vo, D. M. Wall, D. Ring, K. Rajendran, and J. D. Murphy, "Techno-economic analysis of biogas upgrading via amine scrubber, carbon capture and ex-situ methanation," Appl. Energy **212**, 1191 (2018).
[35]M. Van Dael, S. Kreps, A. Virag, K. Kessels, K. Remans, D. Thomas, and F. D. Wilde, "Techno-economic assessment of a microbial power-to-gas plant—Case study in Belgium," Appl. Energy **215**, 416 (2018).
[36]S. Michailos, M. Walker, A. Moody, D. Poggio, and M. Pourkashanian, "Biomethane production using an integrated anaerobic digestion, gasification and CO_2 biomethanation process in a real waste water treatment plant: A techno-economic assessment," Energy Convers. Manag. **209**, 112663 (2020).
[37]See http://www.agronext.iastate.edu/immag/pubs/manure-prod-char-d384-2.pdf for ASAE, ASAE D384.2 MAR2005 Manure Production and Characteristics American Society of Agricultural Engineers, 2005.
[38]See https://www.nyiso.com/custom-reports for New York Independent System Operator, Energy Market and Operational Data Custom Reports, 2020.
[39]See https://www.eia.gov/maps/layer_info-m.php for Energy Information Administration, Layer Information for Interactive State Maps, 2018.
[40]See https://ansci.cals.cornell.edu/about-us/facilities/ for Cornell University College of Agriculture and Life Sciences, Department of Animal Science—Facilities, 2019.
[41]B. E. Rittmann and P. L. McCarty, *Environmental Biotechnology: Principles and Applications* (McGraw-Hill Education, New York, 2001).
[42]J. G. Usack, L. G. Van Doren, R. Posmanik, J. W. Tester, and L. T. Angenent, "Harnessing anaerobic digestion for combined cooling, heat, and power on dairy farms: An environmental life cycle and techno-economic assessment of added cooling pathways," J. Dairy Sci. **102**, 3630 (2019).
[43]I. Ullah Khan, M. Hafiz Dzarfan Othman, H. Hashim, T. Matsuura, A. F. Ismail, M. Rezaei-DashtArzhandi, and I. W. Azelee, "Biogas as a renewable energy fuel—A review of biogas upgrading, utilisation and storage," Energy Convers. Manag. **150**, 277 (2017).
[44]K. H. Hansen, I. Angelidaki, and B. K. Ahring, "Anaerobic digestion of swine manure: Inhibition by ammonia," Water Res. **32**, 5 (1998).
[45]See https://www.extension.uidaho.edu/publishing/pdf/CIS/CIS1215.pdf for University of Idaho Extension, Anaerobic Digestion Basics, 2014.
[46]C. Mao, Y. Feng, X. Wang, and G. Ren, "Review on research achievements of biogas from anaerobic digestion," Renewable Sustainable Energy Rev. **45**, 540 (2015).
[47]L. T. Angenent, J. G. Usack, J. Xu, D. Hafenbradl, R. Posmanik, and J. W. Tester, "Integrating electrochemical, biological, physical, and thermochemical process units to expand the applicability of anaerobic digestion," Bioresour. Technol. **247**, 1085 (2018).
[48]J. G. Usack, L. G. Van Doren, R. Posmanik, R. A. Labatut, J. W. Tester, and L. T. Angenent, "An evaluation of anaerobic co-digestion implementation on New York State dairy farms using an environmental and economic life-cycle framework," Appl. Energy **211**, 28 (2018).
[49]B. Fröschle, M. Heiermann, M. Lebuhn, U. Messelhäusser, and M. Plöchl, in *Biogas Science and Technology*, edited by G. M. Guebitz, A. Bauer, G. Bochmann, A. Gronauer, and S. Weiss (Springer International Publishing, Cham, 2015), pp. 63–99.

[50]F. Vedrenne, F. Béline, P. Dabert, and N. Bernet, "The effect of incubation conditions on the laboratory measurement of the methane producing capacity of livestock wastes," Bioresour. Technol. **99**, 146 (2008).
[51]R. Posmanik, C. M. Martinez, B. Cantero-Tubilla, D. A. Cantero, D. L. Sills, M. J. Cocero, and J. W. Tester, "Acid and alkali catalyzed hydrothermal liquefaction of dairy manure digestate and food waste," ACS Sustainable Chem. Eng. **6**, 2724 (2018).
[52]S. S. Toor, L. Rosendahl, and A. Rudolf, "Hydrothermal liquefaction of biomass: A review of subcritical water technologies," Energy **36**, 2328 (2011).
[53]J. Fang, L. Zhan, Y. S. Ok, and B. Gao, "Minireview of potential applications of hydrochar derived from hydrothermal carbonization of biomass," J. Ind. Eng. Chem. **57**, 15 (2018).
[54]I. Bargmann, M. C. Rillig, A. Kruse, J.-M. Greef, and M. Kücke, "Effects of hydrochar application on the dynamics of soluble nitrogen in soils and on plant availability," J. Plant Nutr. Soil Sci. **177**, 48 (2014).
[55]S. Schimmelpfennig, C. Kammann, G. Moser, L. Grünhage, and C. Müller, "Changes in macro- and micronutrient contents of grasses and forbs following Miscanthus x giganteus feedstock, hydrochar and biochar application to temperate grassland," Grass Forage Sci. **70**, 582 (2015).
[56]S. Abel, A. Peters, S. Trinks, H. Schonsky, M. Facklam, and G. Wessolek, "Impact of biochar and hydrochar addition on water retention and water repellency of sandy soil," Geoderma **202–203**, 183 (2013).
[57]N. Kassem, J. Hockey, C. Lopez, L. Lardon, L. T. Angenent, and J. W. Tester, "Integrating anaerobic digestion, hydrothermal liquefaction, and biomethanation within a power-to-gas framework for dairy waste management and grid decarbonization: A techno-economic assessment," Sustainable Energy Fuels **4**, 4644 (2020).
[58]See https://hydrogeneurope.eu/hydrogen-production-renewables for Hydrogen Europe, Hydrogen Production from Renewables, 2019.
[59]K. Zeng and D. Zhang, "Recent progress in alkaline water electrolysis for hydrogen production and applications," Prog. Energy Combust. Sci. **36**, 307 (2010).
[60]M. Carmo, D. L. Fritz, J. Mergel, and D. Stolten, "A comprehensive review on PEM water electrolysis," Int. J. Hydrogen Energy **38**, 4901 (2013).
[61]M. Lehner, R. Tichler, H. Steinmuller, and M. Koppe, *Power-to-Gas: Technology and Business Models* (Springer International, 2014).
[62]H. Blanco, W. Nijs, J. Ruf, and A. Faaij, "Potential for hydrogen and power-to-liquid in a low-carbon EU energy system using cost optimization," Appl. Energy **232**, 617 (2018).
[63]S. M. Saba, M. Müller, M. Robinius, and D. Stolten, "The investment costs of electrolysis—A comparison of cost studies from the past 30 years," Int. J. Hydrogen Energy **43**, 1209 (2018).
[64]C. Wulf, J. Linßen, and P. Zapp, "Review of power-to-gas projects in Europe," Energy Procedia **155**, 367 (2018).
[65]O. Schmidt, A. Gambhir, I. Staffell, A. Hawkes, J. Nelson, and S. Few, "Future cost and performance of water electrolysis: An expert elicitation study," Int. J. Hydrogen Energy **42**, 30470 (2017).
[66]M. Thema, F. Bauer, and M. Sterner, "Power-to-Gas: Electrolysis and methanation status review," Renewable Sustainable Energy Rev. **112**, 775 (2019).
[67]X. Zhang, S. H. Chan, H. K. Ho, S.-C. Tan, M. Li, G. Li, J. Li, and Z. Feng, "Towards a smart energy network: The roles of fuel/electrolysis cells and technological perspectives," Int. J. Hydrogen Energy **40**, 6866 (2015).
[68]X. Liu, S. Shanbhag, T. V. Bartholomew, J. F. Whitacre, and M. S. Mauter, "Cost comparison of capacitive deionization and reverse osmosis for brackish water desalination," ACS EST Eng. (published online).
[69]See http://www.electrochaea.com/ for Electrochaea GmbH, Electrochaea GmbH Power to Gas Energy Storage, 2019.
[70]T. Schaaf, J. Grünig, M. R. Schuster, T. Rothenfluh, and A. Orth, "Methanation of CO_2—Storage of renewable energy in a gas distribution system," Energy. Sustainable Soc. **4**, 2 (2014).
[71]T. T. Q. Vo, A. Xia, D. M. Wall, and J. D. Murphy, "Use of surplus wind electricity in Ireland to produce compressed renewable gaseous transport fuel through biological power to gas systems," Renewable Energy **105**, 495 (2017).
[72]G. M. Astill, R. C. Shumway, and C. Frear, *Anaerobic Digester System Enterprise Budget Calculator* (Economic Research Service, U.S. Department of Agriculture, 2018).
[73]G. M. Astill and C. R. Shumway, "Profits from pollutants: Economic feasibility of integrated anaerobic digester and nutrient management systems," J. Environ. Manage. **184**, 353 (2016).
[74]See https://www.greenlanerenewables.com/biogas/technology/ for Geenlane Biogas, Biogas Upgrading, 2020.
[75]See https://www.europeanbiogas.eu/greenlane-biogas-order-secured-for-biogas-upgrading-plant-from-sifang-leo-livestock-science-and-technology/ for European Biogas Association, Greenlane Biogas: Order secured for biogas upgrading plant from Sifang Leo Livestock Science and Technology, 2015.
[76]A. A. Peterson, F. Vogel, R. P. Lachance, M. Fröling, M. J. Antal, and J. W. Tester, "Thermochemical biofuel production in hydrothermal media: A review of sub- and supercritical water technologies," Energy Environ. Sci. **1**, 32 (2008).
[77]L. G. Van Doren, R. Posmanik, F. A. Bicalho, J. W. Tester, and D. L. Sills, "Prospects for energy recovery during hydrothermal and biological processing of waste biomass," Bioresour. Technol. **225**, 67 (2017).
[78]R. Posmanik, R. A. Labatut, A. H. Kim, J. G. Usack, J. W. Tester, and L. T. Angenent, "Coupling hydrothermal liquefaction and anaerobic digestion for energy valorization from model biomass feedstocks," Bioresour. Technol. **233**, 134 (2017).
[79]R. Turton, R. C. Bailie, W. Whiting, and J. A. Shaeiwitz, *Analysis, Synthesis and Design of Chemical Processes* (Prentice Hall, New Jersey, 1999).
[80]G. D. Ulrich and P. T. Vasudevan, *Chemical Engineering Process Design and Economics: A Practical Guide*, 2nd ed. (Process Publishing, 2004).
[81]C. Gooch, J. Pronto, B. Gloy, N. Scott, S. McGlynn, and C. Bentley, *Feasibility Study of Anaerobic Digestion and Biogas Utilization Options for the Proposed Lewis County Community Digester* (Cornell University, 2010), available at http://northeast.manuremanagement.cornell.edu/Pages/Funded_Projects/Past_Funded_%20Projects.html.
[82]See https://www.geotab.com/truck-mpg-benchmark/ for Geotab, The State of Fuel Economy in Trucking 2019, 2019.
[83]See https://www.eia.gov/environment/emissions/co2_vol_mass.php for Energy Information Administration—Independent Statistics and Analysis, Carbon Dioxide Emissions Coefficients, 2016.
[84]See https://www.eia.gov/dnav/ng/hist/rngwhhdm.htm for Energy Information Administration, Henry Hub Natural Gas Spot Price, 2019.
[85]See https://www.eia.gov/dnav/ng/ng_pri_sum_a_EPG0_PCS_DMcf_a.htm for Energy Information Administration, Natural Gas Prices, 2018.
[86]See https://www.irena.org/costs/Power-Generation-Costs/Hydropower for International Renewable Energy Agency, Hydropower.
[87]See https://www.irena.org/-/media/Files/IRENA/Agency/Publication/2019/May/IRENA_Renewable-Power-Generations-Costs-in-2018.pdf for International Renewable Energy Agency, Renewable Power Generation Costs in 2018, Abu Dhabi, 2019.
[88]See https://www.eia.gov/outlooks/archive/aeo19/pdf/electricity_generation.pdf for Energy Information Administration—Independent Statistics and Analysis, Levelized Cost and Levelized Avoided Cost of New Generation Resources in the Annual Energy Outlook 2019, 2019.
[89]See https://www.nyserda.ny.gov/Researchers-and-Policymakers/Energy-Prices/Electricity/Monthly-Avg-Electricity-Commercial for New York State Energy Research and Development Authority, Monthly Average Retail Price of Electricity—Commercial, 2020.
[90]See https://www.epa.gov/renewable-fuel-standard-program/overview-renewable-fuel-standard for Environmental Protection Agency, Overview for Renewable Fuel Standard, 2019.
[91]See https://www.epa.gov/renewable-fuel-standard-program/what-fuel-pathway for Environmental Protection Agency, What is a Fuel Pathway?, 2019.
[92]See https://www.epa.gov/fuels-registration-reporting-and-compliance-help/rin-trades-and-price-information for Environmental Protection Agency, RIN Trades and Price Information, 2019.
[93]See https://ww3.arb.ca.gov/fuels/lcfs/background/basics.htm for California Air Resources Board, LCFS Basics, 2019.
[94]J. A. Libra, K. S. Ro, C. Kammann, A. Funke, N. D. Berge, Y. Neubauer, M. M. Titirici, C. Fühner, O. Bens, J. Kern, and K. H. Emmerich, "Hydrothermal carbonization of biomass residuals: A comparative review of the chemistry, processes and applications of wet and dry pyrolysis," Biofuels **2**, 71 (2011).

[95]M. Lucian and L. Fiori, "Hydrothermal carbonization of waste biomass: Process design, modeling, energy efficiency and cost analysis," Energies **10**, 211 (2017).
[96]A. Saba, K. McGaughy, and M. Reza, "Techno-economic assessment of co-hydrothermal carbonization of a coal-miscanthus blend," Energies **12**, 630 (2019).
[97]M. B. Ahmed, J. L. Zhou, H. H. Ngo, and W. Guo, "Insight into biochar properties and its cost analysis," Biomass Bioenergy **84**, 76 (2016).
[98]See https://biochar-international.org/state-of-the-biochar-industry-2013/ for International Biochar Initiative, 2013 State of the Biochar Industry—A Survey of Commercial Activity in the Biochar Field, 2013.
[99]P. Pradhan, P. Gadkari, S. M. Mahajani, and A. Arora, "A conceptual framework and techno-economic analysis of a pelletization-gasification based bio-energy system," Appl. Energy **249**, 1 (2019).
[100]See https://atb.nrel.gov/electricity/2018/index.html?t=cg for National Renewable Energy Laboratory, Natural Gas Plants, 2018.
[101]D. Parra, X. Zhang, C. Bauer, and M. K. Patel, "An integrated techno-economic and life cycle environmental assessment of power-to-gas systems," Appl. Energy **193**, 440 (2017).
[102]See https://www.eia.gov/dnav/ng/NG_CONS_SUM_DCU_SNY_A.htm for Energy Information Administration, Natural Gas Consumption by End Use, 2017.